

Retinoic Acid Potentiates Orbital Tissues for Inflammation Through NF- κ B and MCP-1

Shelby P. Unsworth,¹ Curtis J. Heisel,¹ Christina F. Tingle,¹ Niharika Rajesh,¹ Phillip E. Kish,¹ and Alon Kahana^{1,2}

¹Department of Ophthalmology and Visual Sciences, Kellogg Eye Center, University of Michigan, Ann Arbor, Michigan, United States

²Consultants in Ophthalmic and Facial Plastic Surgery, Southfield, Michigan, United States

Correspondence: Alon Kahana, Department of Ophthalmology and Visual Sciences, Kellogg Eye Center, University of Michigan, 1000 Wall Street, Ann Arbor, MI 48105, USA; alonk123@gmail.com.

Received: March 18, 2020

Accepted: May 27, 2020

Published: July 14, 2020

Citation: Unsworth SP, Heisel CJ, Tingle CF, Rajesh N, Kish PE, Kahana A. Retinoic acid potentiates orbital tissues for inflammation through NF- κ B and MCP-1. *Invest Ophthalmol Vis Sci.* 2020;61(8):17. <https://doi.org/10.1167/iovs.61.8.17>

PURPOSE. The orbit displays unique vulnerability to inflammatory conditions. The most prevalent of these conditions, thyroid eye disease (TED), occurs in up to 50% of patients with Graves' disease (GD). Whereas the pathology of both TED and GD is driven by autoantibodies, it is unclear why symptoms manifest specifically in the orbit.

METHODS. We performed retinoic acid treatment on both normal and TED patient-derived orbital fibroblasts (OFs) followed by mRNA and protein isolation, quantitative real-time polymerase chain reaction (qRT-PCR), enzyme-linked immunosorbent assay, RNA sequencing, and Western blot analyses.

RESULTS. Both normal and TED patient-derived OFs display robust induction of monocyte chemoattractant protein 1 (MCP-1) upon retinoid treatment; TED OFs secrete significantly more MCP-1 than normal OFs. In addition, pretreatment of OFs with thiophenecarboxamide (TPCA-1) inhibits retinoid-induced MCP-1 induction, suggesting an NF- κ B (nuclear factor kappa-light-chain-enhancer of activated B cells)-dependent mechanism. We also found that treatment with cholecalciferol (vitamin D₃) mitigates MCP-1 induction, likely because of competition between retinoic acid receptors (RARs) and vitamin D receptors (VDR) for their common binding partner retinoid nuclear receptors (RXRs).

CONCLUSIONS. Retinoids that naturally accumulate in orbital adipose tissue can act on orbital fibroblasts to induce the expression of inflammation-associated genes. These data suggest a potential role for retinoids in sensitizing the orbit to inflammation.

Keywords: inflammation, orbit, thyroid eye disease, Graves, pseudotumor

Although the eye displays immune privilege¹ (reviewed in²), the eye socket (i.e., orbit) is highly vulnerable to inflammation.³ Orbital inflammatory conditions include thyroid eye disease (TED),^{4,5} lupus, polyangiitis with granulomatosis, sarcoidosis, Sjogren, immunoglobulin G4-associated disease, orbital myositis, histiocytic disorders, and xanthogranuloma.³ Nonspecific orbital inflammation (NSOI) is also very common, representing 50% of orbital inflammatory conditions. Inflammatory masses, referred to as "orbital pseudotumor," represent 8% to 10% of all orbital masses.⁶ Other systemic autoimmune or inflammatory conditions such as rheumatoid arthritis^{7,8} and inflammatory bowel disease⁹ can also affect the orbit. This represents a remarkable list of orbital inflammatory conditions essentially unmatched elsewhere in the body. Orbital inflammation causes a range of symptoms including redness, pain, swelling, and decreased vision; however, the mechanism underlying orbital sensitivity to inflammation is unclear.

TED is the most prevalent cause of orbital inflammation, occurring in up to 50% of patients with Graves' disease (GD).¹⁰ Although the biology underlying GD is understood,^{10–12} the mechanism of the orbitopathy remains ambiguous. The current prevailing hypothesis is that autoan-

tibodies bind thyrotropin (TSHR) and insulin-related growth factor (IGF-1R) receptors expressed on orbital fibroblasts (OFs) to promote local inflammation.¹³ However, autoantibody animal models do not fully recapitulate human TED and do not address the mechanism of orbital specificity given that TSHR and IGR-1R are expressed throughout the body.

One unique attribute of orbital tissue is the presence of carotenoids stored in orbital fat,¹⁴ presumably a byproduct of retinoic acid's role in visual transduction and orbital biology.^{15–17} Here, we show that retinoids are present in orbital adipose tissues obtained from both normal and TED patients. In addition, OFs treated with all-*trans* retinoic acid (ATRA) and 9-*cis* retinoic acid (9CRA) induce expression of a variety of inflammation-associated genes, including monocyte chemoattractant protein-1 (MCP-1), a previously identified key regulator of TED pathogenesis.^{18–20} This MCP-1 induction is dependent on NF- κ B (nuclear factor kappa-light-chain-enhancer of activated B cells), because treatment with thiophenecarboxamide (TPCA-1), a potent inhibitor of I κ B kinase (IKK) 2, mitigates MCP-1 expression. Interestingly, treatment of OFs with cholecalciferol (vitamin D₃) also mitigates MCP-1 expression, consistent with the potential

link between vitamin D deficiency and TED pathogenesis.²¹ This is potentially due to competitive binding of vitamin D receptor (VDR) to retinoid nuclear receptors (RXRs), which are required for retinoic acid receptor (RAR) signaling.²² Taken together, these data suggest that retinoids stored in orbital adipose tissue may sensitize the orbit to inflammation and highlight retinoid signaling as a potential therapeutic target for orbital inflammatory conditions.

METHODS

Primary Orbital Fibroblast Culture

Orbital fat was collected from Graves' and normal patients during orbital decompression or blepharoplasty. Informed consent was obtained and study was performed in compliance with the University of Michigan Institutional Review Board (HUM00142787). After collection, 1 to 2 mL of fat was washed with Dulbecco's phosphate-buffered saline (PBS) and placed in a 15-cm dish containing OF growth media (Dulbecco's modified Eagle medium [DMEM] culture media supplemented with 10% fetal bovine serum, 1% HEPES, 2.5% sodium pyruvate, and 0.2% primocin antibiotic). Media was changed every seven days until plates reached sub-confluence (~4 weeks), on which P1 and P2 cells were used for experiments.

Retinoid, TPCA-1, and Vitamin D Treatments for Gene Expression Analysis

Before treatment, OF growth media was removed, and cells were washed with "no serum" media (DMEM culture media supplemented with 1% HEPES, 2.5% sodium pyruvate, and 0.2% primocin antibiotic). For gene expression analysis after retinoid treatment, cells were treated with varying concentrations of all-trans retinoic acid (ATRA) or 9-cis retinoic acid (9CRA) in "no serum" media. After six hours, media was removed, cells were collected in 2 mL Trizol solution (Ambion, Austin, TX, USA), and RNA was isolated using the ReliaPrep RNA tissue Miniprep System (Promega, Madison, WI, USA). The cDNA was synthesized using iScript Reverse Transcriptase Supermix (Bio-rad, Hercules, CA, USA), and all qRT-PCR experiments were run in triplicate using 2× SYBR Green qPCR master mix (bimake.com). The qRT-PCR primer sequences are shown in Supplementary Table S1. Gene expression relative to RPS13 was performed, and fold-change in expression was determined by normalizing to the dimethylsulfoxide (DMSO)-treated samples. For vitamin D experiments, cells were treated with either DMSO alone, 100 nmol/L D3 (cholecalciferol), 1 μmol/L ATRA, or both 100 nmol/L D3, and 1 μmol/L ATRA for six hours before collection. For TPCA-1 experiments, cells were pretreated with either DMSO or 1 μmol/L TPCA-1 for 30 to 45 minutes, followed by treatment with DMSO or 1 μmol/L ATRA for an additional 5.5 hours before collection. RNA isolation, cDNA synthesis, and qRT-PCR was performed as previously described.

ELISA Assessment of MCP-1 Secretion

On confluence, cells were washed once with "no-serum" media and then treated with "no-serum" media containing either DMSO or 1 μmol/L ATRA for 48 hours, after which media was collected and stored at -80°C. Enzyme-linked immunosorbent assay (ELISA) experiments were performed

using the Invitrogen CCL2 Uncoated ELISA kit according to the kit protocol with an N of 6.

Immunofluorescence Staining of Cultured Orbital Fibroblasts

OFs were grown to confluence in OF growth media in 15-cm plates containing three or four glass slides. On confluence, cells were treated with DMSO or ATRA as previously described. After treatment, slides were immediately fixed in 4% PFA for 15 minutes followed by three washes in PBS-Tween 0.2, one wash with PBS-Triton 0.5%, followed by a final wash in PCR-Tween 0.2%. Blocking was performed using 20% normal goat serum for 30 minutes followed by overnight incubation in primary antibody diluted in 5% NGS/PBS-Tween 0.2% (NF-κB p65 [D14E12] rabbit mAb, 1:1000; Cell Signaling Technology, Danvers, MA, USA). The following day, slides were washed three times with PBS-Tween 0.2% followed by a one-hour incubation in secondary antibody (Goat Anti-Rabbit Alexa Fluor 555, 1:300, Invitrogen, Carlsbad, CA, USA) in 5% NGS/PBS-Tween 0.2%. Slides were washed an additional three times in PBS-Tween 0.2% before mounting with Prolong Gold containing DAPI (Invitrogen).

RA Extraction and Mass Spectrometry Analysis

The all-trans retinol and all-trans retinoic acids were obtained from Sigma (St. Louis, MO, USA). The d6-all-trans retinol and d6-all-trans retinoic acids were purchased from Cambridge Isotopes Laboratories (Andover, MA, USA). All compounds were stored in amber vials in ethanol as 1 mg/mL stocks at -20°C. Acetonitrile, methanol, water, and formic acid used in the UHPLC-MS/MS method were from Fischer Scientific (Pittsburg, PA, USA), and all were Optima LC/MS grade.

Retinoids were extracted by homogenization in solvent using a probe sonicator (Branson 450, duty cycle 40%, output power level 4). Biological samples were homogenized in 4:1:7 MeOH: H₂O: Hexane containing deuterated internal standards d6-all trans retinol and d6-all trans retinoic acid. The homogenate was centrifuged at 15,000g for 10 minutes and the top hexane layer was transferred to the auto sampler vial, dried under N₂ and reconstituted with 100 μL 40:60 H₂O: ACN for mass spectrometry analysis.

The dried extracts were injected onto an Acquity CSH C18 1.7 μm 2.1 × 100 mm column (Waters, Milford, MA, USA) that was heated to 40°C. A binary gradient system was used; eluent A was water with 0.1% formic acid and eluent B was acetonitrile with 0.1% formic acid. The gradient profile consisted of the following: linear ramp from 100% A to 95% B from zero to seven minutes, hold 95% B between seven to 28 minutes, return to 100% A from 28 to 28.1 minutes, and hold 100%A from 28.1 to 35 minutes. The flow rate was 0.250 mL/min and the sample injection volume was 10 μL. Pooled human plasma and master pools were used as quality controls. Master pools made from a small aliquot from all samples were injected at the beginning, end, and at regular intervals throughout each analysis batch to provide a measurement of the system's stability and performance.

ESI-MS/MS data acquisition was performed in positive ion mode using an Agilent 6490 QQQ-LC-MS with multiple reaction monitoring (MRM) transitions programmed for both labeled and unlabeled internal standards. MRM

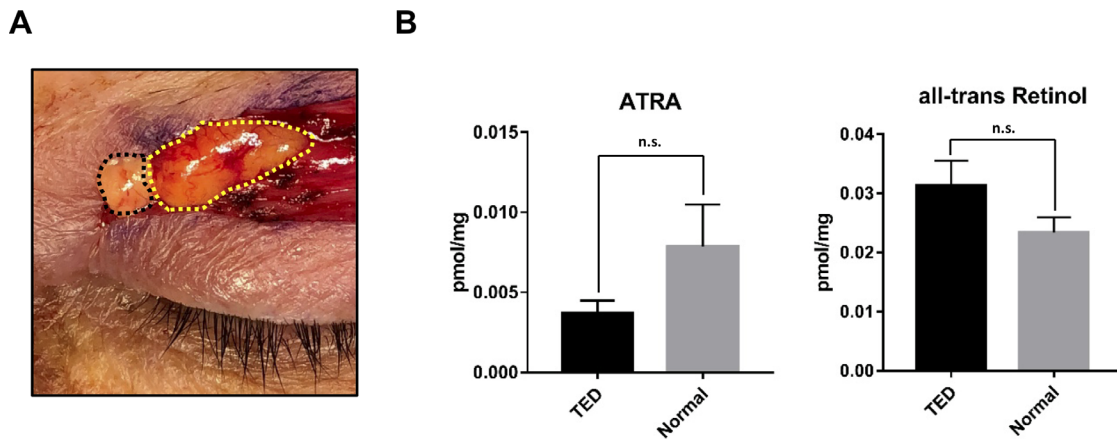


FIGURE 1. Retinoids are present in orbital fat. (A) Preaponeurotic orbital fat (yellow outline) displays a distinct yellow/orange color when compared to nasal fat (black outline). (B) ATRA (left panel) and all-trans retinol (right panel) are present in orbital fat from both normal (N = 7) and TED (N = 8) patients. (Error bars: SEM)

transitions for target retinoids were: 269 > 91 (native all trans retinol) and 275 > 96 (labeled all trans retinol), 301 > 91 (native ATRA) and 307 > 96 (d6-ATRA). Quantitation was performed by isotope dilution mass spectrometry using native/labeled peak area ratios. LC-MS data were processed using MassHunter Quantitative Analysis software version B.08.00. For tissues the quantitative data were normalized to tissue weight and were reported as picomoles per milligram tissue. For cell lysates samples the quantitative data are reported as nanomoles per liter.

Transcriptome Analysis

Sequencing was performed by the UM Advanced Genomics Core (AGC), with Quant-seq libraries constructed and subsequently subjected sequencing. Raw data were then processed by the AGC to generate a raw count table of all genes for each sample, using UCSC hg19. Quality control and sequence alignment At the UM Bioinformatics Core, we downloaded the reads and count summary files from the Advanced Genomics Core's storage. FastQC results were reviewed to ensure that only high-quality data were used for expression quantitation and differential expression. Differential Expression Data were prefiltered to remove genes with less than 10 counts in all samples. Differential gene expression analysis was performed using DESeq2,²³ using a negative binomial generalized linear model with a term to account for "PatientOrigin" (thresholds: linear fold change >1.5 or <-1.5, Benjamini-Hochberg FDR [Padj] <0.05). Plots were generated using variations of DESeq2 plotting functions and other packages with R version 3.3.3. Genes were annotated with NCBI Entrez GeneIDs and text descriptions. Functional analysis, including candidate pathways activated or inhibited in comparison(s) and GO-term enrichments, was performed using iPathway Guide (Advaita).

Statistics

Repeat-measures one-way analysis of variance (ANOVA) and Student's paired *t*-tests were performed in GraphPad Prism 7.00 to determine variance and statistical significance between treatment groups. All gene expression experiments were performed with an N of at least 5 (OFs from distinct patients).

RESULTS

Retinoids in Orbital Adipose Tissue

The distinct color difference between preaponeurotic orbital and nasal fat is attributed to increased presence of carotenoids (Fig. 1A).²⁴ To assess which specific retinoid species are present in orbital fat, we performed mass spectrometry on orbital fat samples isolated from both normal and TED patients. The mean ATRA concentration was 0.0037 pmol/ μ g in TED samples and 0.0079 pmol/ μ g in normal samples; however, this difference was not statistically significant ($P = 0.13$, Fig. 1B). All-trans retinol was also present in higher concentrations in both samples (0.031 in TED, 0.023 in normal, $P = 0.14$, Fig. 1B).

Retinoids Promote Inflammatory Cytokine Expression in Orbital Fibroblasts

The presence of retinoids in orbital fat led us to question their effect on resident orbital fibroblasts. To test this, we treated primary OFs with 0.01, 0.1, 1, and 10 μ mol/L ATRA and 9CRA. We found that both ATRA and 9CRA treatment resulted in a dose-dependent induction of the inflammatory cytokine monocyte chemoattractant protein-1 (MCP-1) (Figs. 2A, 2B). A 1- μ mol/L dosage for both 9CRA and ATRA showed maximal induction, so that concentration was used for all future experiments. In addition to MCP-1, we also looked at the effect of ATRA treatment on other TED-associated genes and found significant induction of versican ($P = 0.03$) and interleukin-1 beta (IL-1 β) ($P = 0.02$), and significant reduction in nuclear factor erythroid 2-related factor 2 ($P = 0.0098$) that regulates expression of antioxidant proteins²⁵ (Supplemental Fig. S1). We then compared ATRA-induced MCP-1 induction in normal versus TED-derived OFs and found that whereas both showed a significant increase in mRNA expression (Fig. 2C), TED-derived OFs displayed significantly more MCP-1 protein secretion compared with normal OFs (Fig. 2D). In addition to MCP-1, ATRA treatment also induced expression of the retinoic acid receptors RAR β and RAR γ , but not RAR α (Fig. 2D) and inhibited expression of thyroid hormone receptors TR α and TR β (Supplemental Fig. S2).

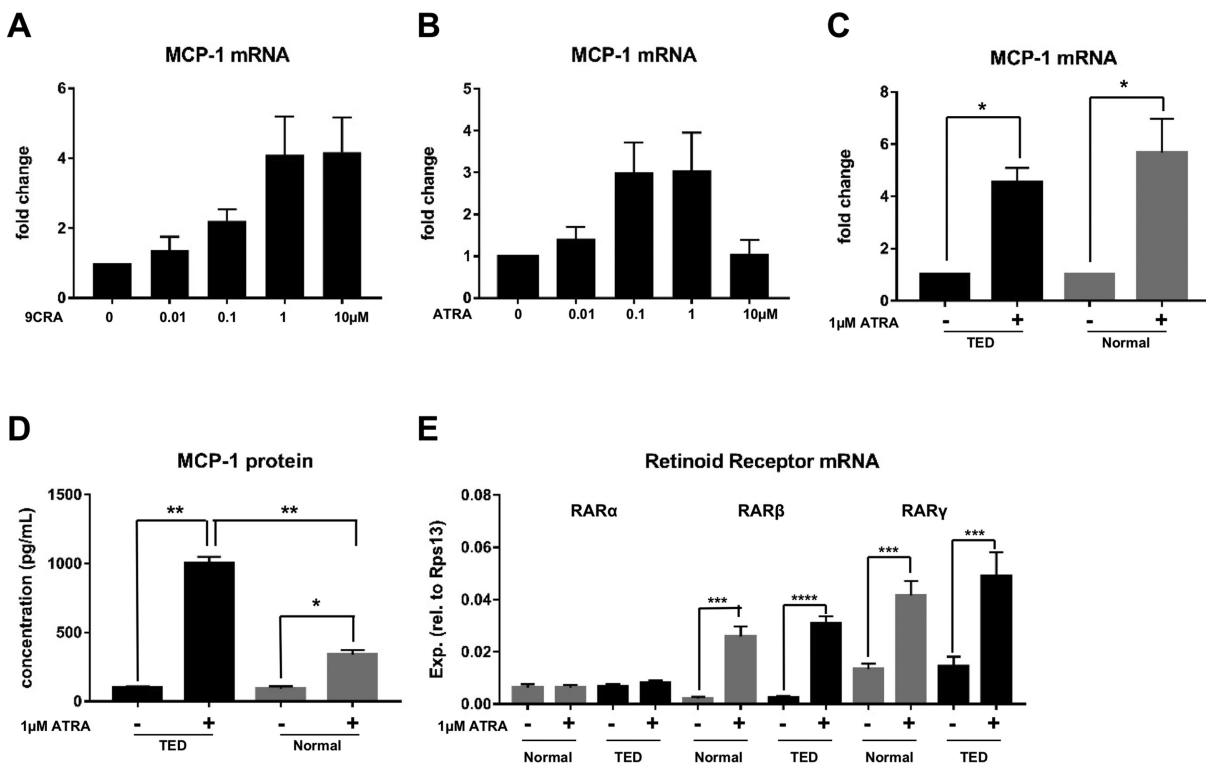


FIGURE 2. Retinoic acid treatment promotes MCP-1 induction in orbital fibroblasts. (A) Dose response of MCP-1 expression upon 9-cis retinoic acid treatment in OFs (RM one-way ANOVA $P = 0.0272$, $N = 5$). (B) Dose response of MCP-1 expression upon ATRA treatment in OFs (RM one-way ANOVA $P = 0.0389$, $N = 6$). (C) ATRA treatment promotes significant induction of MCP-1 expression in both normal ($N = 6$) and TED OFs ($N = 7$). (D) ATRA treatment promotes MCP-1 secretion in both normal and TED OFs, TED OFs show increased secretion compared with normal OFs ($N = 3$). (E) ATRA treatment promotes expression of retinoic acid receptors (RAR) α and β ($N = 8$). (* $P < 0.05$, ** $P < 0.01$, *** $P < 0.001$, **** $P < 0.0001$).

MCP-1 Induction Is NF- κ B Dependent

MCP-1 is a known modulator of orbital inflammation.^{20,26} Many factors induce MCP-1 expression in vitro, including tissue plasminogen activator,²⁷ lipopolysaccharide,²⁸ IL-1 β ,²⁹ tumor necrosis factor- α ,²⁹ platelet-derived growth factor,³⁰ interferon gamma,³¹ and interleukin-17 (IL-17).³² All of these factors promote MCP-1 expression primarily via activation of the transcription factor complex NF- κ B (nuclear factor kappa-light-chain-enhancer of activated B cells).

Functional interaction between NF- κ B and the retinoic acid (RA) pathway has been established in several different cell types. In endothelial cells, adjacent NF- κ B and RA response elements are required for synergistic transcriptional regulation of ICAM-1.³³ In keratinocytes, RA promotes expression of interleukin-8 (IL-8) in an NF- κ B dependent manner.³⁴ ATRA has also been shown to induce NF- κ B activation via phosphorylation and subsequent degradation of I κ B.³⁴ In OFs, ATRA treatment promotes phosphorylation and nuclear translocation of the NF- κ B p65 subunit (Figs. 3A, 3B).

To test whether ATRA-induced MCP-1 expression is NF- κ B dependent, we used TPCA-1, a potent IKK inhibitor that prevents phosphorylation and subsequent degradation of the inhibitory protein I κ B α .³⁵ We treated OFs with 1 μ mol/L TPCA-1 for 30 minutes before ATRA treatment and found that TPCA-1 significantly inhibited MCP-1 induction (Fig. 3C).

Dermal Fibroblasts Display NF- κ B Dependent MCP-1 Induction

To assess whether the observed ATRA response is unique to OFs, we performed ATRA treatment on primary human dermal fibroblasts (DF). We found that upon ATRA treatment, DFs significantly induce expression of MCP-1 (Supplemental Fig. S3A, $P = 0.0001$). This induction is also NF- κ B dependent, because pretreatment with TPCA-1 inhibits MCP-1 induction (Supplemental Fig. S3B, $P = 0.0038$).

Vitamin D₃ Treatment Mitigates MCP-1 Induction

Retinoic acid receptors (RAR) belong to a superfamily of nuclear receptors, which heterodimerize with retinoid nuclear receptors (RXR) and bind DNA to influence transcription.^{36–38} Vitamin D receptor (VDR) belongs to the same superfamily and also requires RXR heterodimerization²² (Fig. 4A). We predicted that vitamin D (D3) treatment may inhibit the effect of ATRA, because D3 has previously been shown to inhibit RA target genes.^{39,40} To test this hypothesis, we treated OFs with both 1 μ mol/L ATRA and 100 nmol/L D3 and found that D3 treatment partially mitigates MCP-1 expression (Fig. 4B, $P = 0.02$). These data are consistent with our recent study, which linked low serum vitamin D levels to TED incidence in GD patients²¹ and suggest that achieving high-normal vitamin D levels via supplementation may be protective against orbital inflammation.

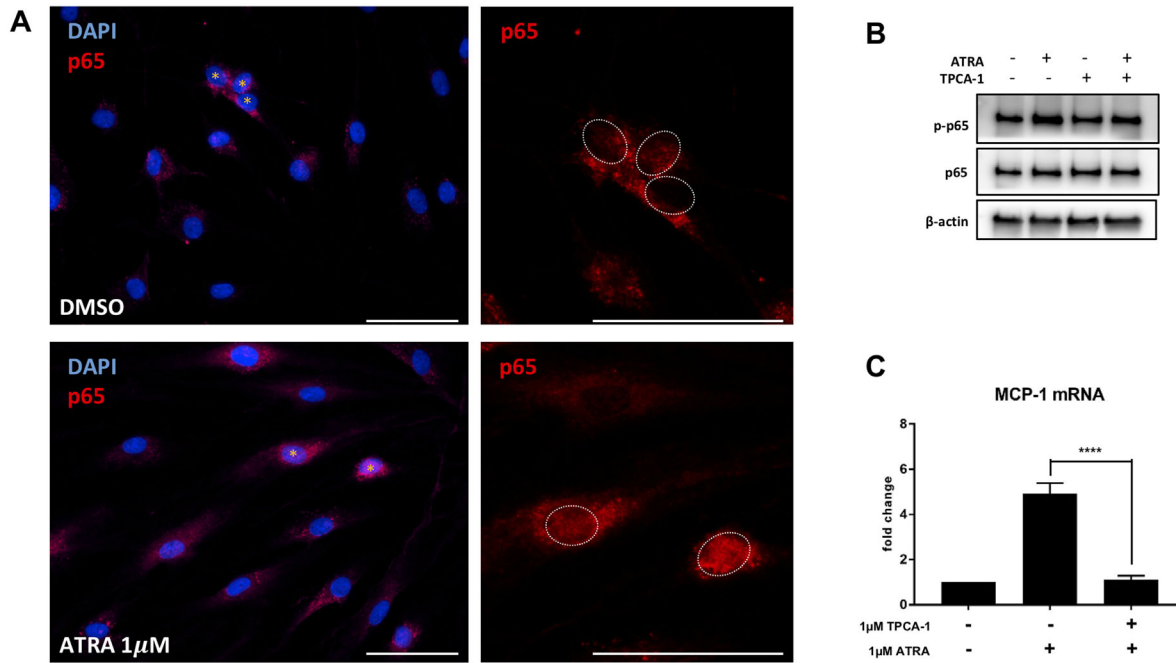


FIGURE 3. MCP-1 induction is NFκB dependent. (A) Increased nuclear (left panel - yellow asterisk, right panel—white outline) expression of p65 (red) in ATRA (bottom panels) versus DMSO (top panels) treated TED OFs (scale bars: 100 μm). (B) TPCA-1 treatment mitigates ATRA-dependent p65 phosphorylation. (C) 1 μmol/L TPCA-1 treatment mitigates ATRA response in OFs (N = 9) (*****P* < 0.0001, error bars: SEM).

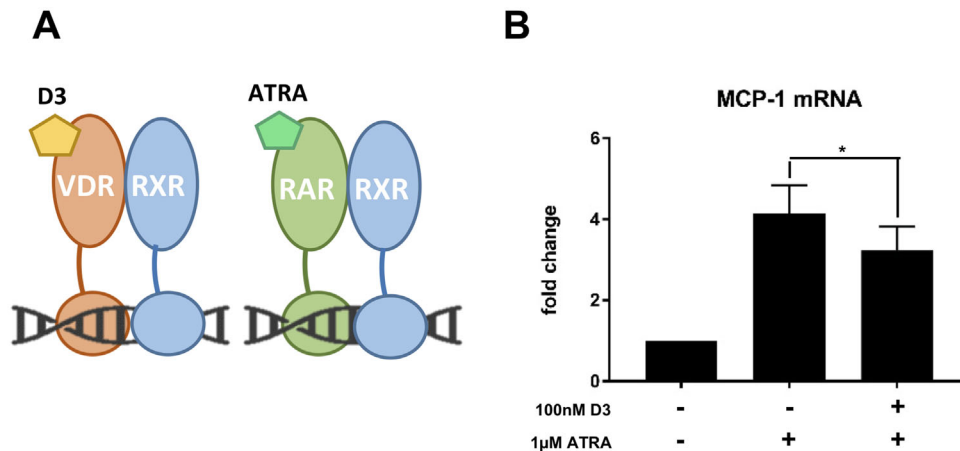


FIGURE 4. Vitamin D partially inhibits MCP-1 induction. (A) Schematic of vitamin D and retinoic acid receptor heterodimerization with retinoid × receptors. (B) Vitamin D treatment inhibits MCP-1 induction in ATRA-treated OFs (N = 5). (**P* < 0.05, error bars: SEM).

ATRA Treatment Promotes Similar Gene Expression Changes in Normal and TED OFs

After observing gene expression changes in TED-associated genes upon ATRA treatment, we next sought to uncover additional pathways affected by ATRA. To do this, we performed 3' RNA sequencing (Quantseq) on both TED and normal OFs treated with DMSO (control) or 1 μmol/L ATRA. We first compared TED and normal DMSO-treated OFs to assess the baseline differences between the two patient populations and found 29 significantly differentially expressed genes (Fig. 5A). We then looked at DMSO versus ATRA treatment in each of our two patient populations.

We found that ATRA treatment resulted in significant differential expression of 221 genes in TED OFs and 199 genes in normal OFs, 130 of which were differentially expressed in both populations (Fig. 5A). Top differentially expressed genes displayed similar expression patterns for both populations, suggesting despite differences at baseline, the two populations respond similarly to ATRA treatment (Fig. 5C). In addition, genes that are differentially expressed at baseline (DMSO) maintain their expression pattern upon ATRA treatment (Fig. 5B), suggesting these genes are not affected by ATRA treatment. Interestingly, although MCP-1 expression was induced in 16 of 19 patients, these changes were not significant. This is potentially due to

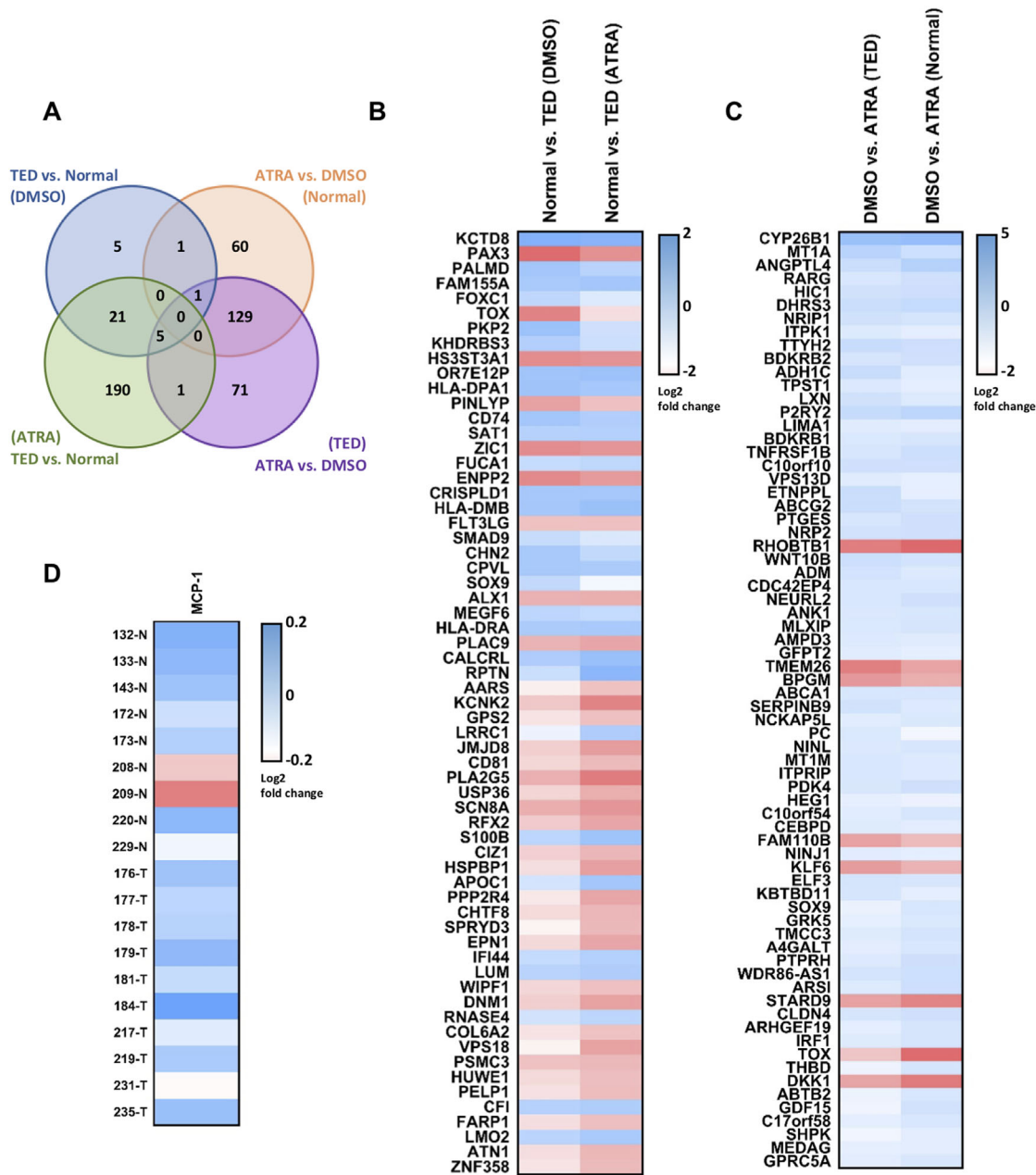


FIGURE 5. ATRa treatment promotes gene expression changes in normal and TED OFs. **(A)** Overlap of differentially expressed genes in TED versus normal DMSO-treated (*blue*) and ATRa-treated (*green*) and ATRa versus DMSO-treated OFs from TED (*purple*) and normal (*orange*) patients. **(B)** Top differentially expressed genes in normal versus TED DMSO (left) and ATRa (right) treated OFs. **(C)** Top differentially expressed genes in ATRa versus DMSO TED (left) and normal (right) OFs. **(D)** MCP-1 expression in ATRa-treated normal (N) and TED (T) OFs.

limited sensitivity of the Quantseq assay, which only maps 3' reads and has been shown to be less sensitive than whole transcript RNAseq.⁴¹ The quantitative real-time polymerase chain reaction (qRT-PCR) assay used in previous figures to highlight MCP-1 expression changes provides a more sensitive and accurate picture of MCP-1 gene expression.

DISCUSSION

Inflammatory conditions represent a major disease burden worldwide. Autoimmune conditions are common, and tissue

damage may be caused by either auto-antibodies specific to an antigen unique to the diseased tissue, such as Graves' disease, or more commonly as "collateral damage" without a clear pathogenic signal, such as thyroid-associated orbitopathy or rheumatoid arthritis. The ocular orbit and the tissues contained therein, for example, muscles, nerves, connective and adipose tissues, are particularly vulnerable to systemic autoimmune inflammatory conditions that seemingly have nothing in common with one another or with orbital tissues. A key question is: Why is the orbit uniquely vulnerable to inflammation?

Orbital tissues contain retinoids. This is likely due to their proximity to the eye, which synthesizes, uses, and recycles retinoids.¹⁵ We hypothesize that the retinoids stored in orbital fat are produced in the eye and diffuse through the sclera. Given the unique predisposition of orbital tissues to inflammation and the finding that orbital tissues are a depot for retinoids, we hypothesized that retinoids may sensitize the orbit to inflammation by promoting expression of inflammatory cytokines. Expression of inflammatory cytokines may prime orbital tissues for invasion by circulating T cells and macrophages associated with a pre-existing systemic inflammatory condition. The most common orbital inflammatory disease is thyroid eye disease (TED), also known as thyroid-associated orbitopathy (TAO). TED patients with a more severe disease course may require orbital decompression surgery, which often includes removal of orbital fibrous and adipose tissues. This provided an opportunity to study fibroblasts and preadipocytes that originate from the orbits of patients with TED. As a control, we used fibroadipose tissue from the superior medial orbital fat pad—a source of fibroblasts that has been shown to be otherwise similar to fibroblasts from the deep orbit.⁴²

In this article, we describe our finding that RA treatment of orbital fibroblasts leads to expression and secretion of MCP-1, a cytokine implicated in the pathogenesis of TED.^{18–20} Whereas RA treatment of both control and TED fibroblasts resulted in MCP-1 induction, fibroblasts from TED patients demonstrated increased MCP-1 secretion in response to RA. MCP-1 induction occurred through the NF- κ B pathway, as blocking NF- κ B inhibited MCP-1 induction. This provides a new biological framework for understanding the susceptibility of orbital tissues to inflammation, which might lead to novel therapies that target the proinflammatory role of the retinoid pathway.

It is important to note that RA-induced cytokine expression occurred in fibroblasts irrespective of their origin, orbital or dermal. Interestingly, both the orbit and the skin are targeted by autoimmune thyroid disease, in the form of the orbitopathy and dermopathy.⁴³ Severe form of the dermopathy is known as pretibial myxedema. In the skin, RA also plays a critical physiologic role in maintaining dermal appendages and regulating epithelial turnover.⁴⁴ Hence, our findings suggest that RA may be a common mechanism through which orbital and dermal tissues are primed de novo for involvement in autoimmune conditions. Indeed, dermatologic inflammatory conditions are extremely common.

Retinoic acid receptors belong to a family of nuclear receptors that include thyroid hormone receptor and vitamin D receptor. Both of these receptors compete with RA receptors for heterodimerization with RXR, a requirement for DNA binding.²² Interestingly, vitamin D deficiency is an independent risk factor for the development of TED.²¹ To test whether vitamin D can block the proinflammatory RA response, we treated OFs with both RA and vitamin D. Indeed, MCP-1 induction was partially inhibited in the presence of vitamin D, providing a potential mechanistic explanation for the clinical association. Our findings suggest that avoidance of vitamin D deficiency and maintaining high-normal serum vitamin D levels through supplementation may have broad protective effects against orbital inflammation.

RA receptors are major regulators of genomic architecture, chromatin structure, and gene expression. To further characterize the OF response to RA treatment, we performed

a transcriptome analysis to identify key pathways affected by RA signaling. We identified 221 differentially expressed genes in TED orbital fibroblasts, and 199 genes in control fibroblasts, after treatment with RA. Interestingly, 130 genes were differentially expressed in both populations of cells, revealing that the response to RA is a fundamental property of orbital fibroblasts and not a byproduct of the disease state. Future studies will aim to dissect these pathways to identify opportunities at targeted therapy that would safely suppress the proinflammatory RA signals.

In summary, these data provide the first mechanistic explanation for the unique susceptibility of orbital tissues to inflammation. The RA pathway is highly amenable to pharmacologic manipulation, including the use of retinoid analogs. The finding that vitamin D can reduce the inflammatory response in OFs and that vitamin D deficiency is a clinical risk factor suggests that therapy focused on this pathway carries significant promise for preventing orbital inflammation in TED and other inflammatory conditions.

Acknowledgments

The authors thank the expert technical assistance of Clara Kim, Daniel Kasprick, and Yi Zhao. The authors thank Francois Rubright of Clermont, Florida, for her generous gift in support of this research.

Supported by Research to Prevent Blindness, Inc. (RPB) via a Medical Student Award from to CJH, a Physician Scientist Award to AK, and an unrestricted grant to the Department of Ophthalmology and Visual Sciences at the University of Michigan. Additional funding was provided by the A. Alfred Taubman Medical Research Institute at the University of Michigan.

Disclosure: **S.P. Unsworth**, None; **C.J. Heisel**, None; **C.F. Tingle**, None; **N. Rajesh**, None; **P.E. Kish**, None; **A. Kahana**, None

References

1. Medawar PB. Immunity to homologous grafted skin; the fate of skin homografts transplanted to the brain, to subcutaneous tissue, and to the anterior chamber of the eye. *Br J Exp Pathol.* 1948;29:58–69.
2. Streilein JW. Ocular immune privilege: therapeutic opportunities from an experiment of nature. *Nat Rev Immunol.* 2003;3:879–889.
3. Gordon LK. Orbital inflammatory disease: a diagnostic and therapeutic challenge. *Eye (Lond).* 2006;20:1196–1206.
4. Bahn RS. Clinical review 157: pathophysiology of Graves' ophthalmopathy: the cycle of disease. *J Clin Endocrinol Metab.* 2003;88:1939–1946.
5. Wall JR. Graves' disease is a multi-system autoimmune disorder in which extra ocular muscle damage and connective tissue inflammation are variable features. *Thyroid.* 2002;12:35–36.
6. Shields JA, Shields CL, Scartozzi R. Survey of 1264 patients with orbital tumors and simulating lesions: The 2002 Montgomery Lecture, part 1. *Ophthalmology.* 2004;111:997.
7. Nabili S, McCarey DW, Browne B, Capell HA. A case of orbital myositis associated with rheumatoid arthritis. *Ann Rheum Dis.* 2002;61:938–939.
8. Panfilio CB, Hernandez-Cossio O, Hernandez-Fustes OJ. Orbital myositis and rheumatoid arthritis: case report. *Arq Neuropsiquiatr.* 2000;58:174–177.
9. Thomas AS, Lin P. Ocular manifestations of inflammatory bowel disease. *Curr Opin Ophthalmol.* 2016;27:552–560.

10. Bahn RS, Heufelder AE. Pathogenesis of Graves' ophthalmopathy. *N Engl J Med*. 1993;329:1468–1475.
11. McIver B, Morris JC. The pathogenesis of Graves' disease. *Endocrinol Metab Clin North Am*. 1998;27:73–89.
12. Perros P, Kendall-Taylor P. Pathogenesis of thyroid-associated ophthalmopathy. *Trends Endocrinol Metab*. 1993;4:270–275.
13. Khong JJ, McNab AA, Ebeling PR, Craig JE, Selva D. Pathogenesis of thyroid eye disease: review and update on molecular mechanisms. *Br J Ophthalmol*. 2016;100:142–150.
14. Sires BS, Saari JC, Garwin GG, Hurst JS, van Kuijk FJ. The color difference in orbital fat. *Arch Ophthalmol*. 2001;119:868–871.
15. von Lintig J. Metabolism of carotenoids and retinoids related to vision. *J Biol Chem*. 2012;287:1627–1634.
16. Bohnsack BL, Kahana A. Thyroid hormone and retinoic acid interact to regulate zebrafish craniofacial neural crest development. *Dev Biol*. 2013;373:300–309.
17. Kish PE, Bohnsack BL, Gallina D, Kasprick DS, Kahana A. The eye as an organizer of craniofacial development. *Genesis*. 2011;49:222–230.
18. Chen MH, Chen MH, Liao SL, Chang TC, Chuang LM. Role of macrophage infiltration in the orbital fat of patients with Graves' ophthalmopathy. *Clin Endocrinol (Oxf)*. 2008;69:332–337.
19. Elner VM, Burnstine MA, Kunkel SL, Strieter RM, Elner SG. Interleukin-8 and monocyte chemoattractant protein-1 gene expression and protein production by human orbital fibroblasts. *Ophthalmic Plast Reconstr Surg*. 1998;14:119–125.
20. Hwang CJ, Afifiyan N, Sand D, et al. Orbital fibroblasts from patients with thyroid-associated ophthalmopathy overexpress CD40: CD154 hyperinduces IL-6, IL-8, and MCP-1. *Invest Ophthalmol Vis Sci*. 2009;50:2262–2268.
21. Heisel CJ, Riddering AL, Andrews CA, Kahana A. Serum vitamin D deficiency is an independent risk factor for thyroid eye disease. *Ophthalmic Plast Reconstr Surg*. 2020;36:17–20.
22. Lefebvre P, Benomar Y, Staels B. Retinoid X receptors: common heterodimerization partners with distinct functions. *Trends Endocrinol Metab*. 2010;21:676–683.
23. Love MI, Huber W, Anders S. Moderated estimation of fold change and dispersion for RNA-seq data with DESeq2. *Genome Biol*. 2014;15:550.
24. Sires BS, Saari JC, Garwin GG, Hurst JS, van Kuijk FJ. The color difference in orbital fat. *Arch Ophthalmol*. 2001;119:868–871.
25. Ma Q. Role of nrf2 in oxidative stress and toxicity. *Annu Rev Pharmacol Toxicol*. 2013;53:401–426.
26. Wakelkamp IM, Bakker O, Baldeschi L, Wiersinga WM, Prummel MF. TSH-R expression and cytokine profile in orbital tissue of active vs. inactive Graves' ophthalmopathy patients. *Clin Endocrinol (Oxf)*. 2003;58:280–287.
27. Shyy YJ, Li YS, Kolattukudy PE. Structure of human monocyte chemoattractant protein gene and its regulation by TPA. *Biochem Biophys Res Commun*. 1990;169:346–51.
28. Rovin BH, Dickerson JA, Tan LC, Hebert CA. Activation of nuclear factor-kappa B correlates with MCP-1 expression by human mesangial cells. *Kidney Int*. 1995;48:1263–1271.
29. Gordon HM, Kucera G, Salvo R, Boss JM. Tumor necrosis factor induces genes involved in inflammation, cellular and tissue repair, and metabolism in murine fibroblasts. *J Immunol*. 1992;148:4021–4027.
30. Cochran BH, Reffel AC, Stiles CD. Molecular cloning of gene sequences regulated by platelet-derived growth factor. *Cell*. 1983;33:939–947.
31. Grandaliano G, Valente AJ, Rozek MM, Abboud HE. Gamma interferon stimulates monocyte chemoattractant protein (MCP-1) in human mesangial cells. *J Lab Clin Med*. 1994;123:282–289.
32. Fang S, Huang Y, Wang S, et al. IL-17A exacerbates fibrosis by promoting the proinflammatory and profibrotic function of orbital fibroblasts in TAO. *J Clin Endocrinol Metab*. 2016;101:2955–2965.
33. Chadwick CC, Shaw LJ, Winneker RC. TNF-alpha and 9-cis-retinoic acid synergistically induce ICAM-1 expression: evidence for interaction of retinoid receptors with NF-kappa B. *Exp Cell Res*. 1998;239:423–429.
34. Dai X, Yamasaki K, Shirakata Y, Sayama K, Hashimoto K. All-trans-retinoic acid induces interleukin-8 via the nuclear factor-kappaB and p38 mitogen-activated protein kinase pathways in normal human keratinocytes. *J Invest Dermatol*. 2004;123:1078–1085.
35. Podolin PL, Callahan JF, Bolognese BJ, et al. Attenuation of murine collagen-induced arthritis by a novel, potent, selective small molecule inhibitor of IκB kinase 2, TPCA-1 (2-[(aminocarbonyl)amino]-5-(4-fluorophenyl)-3-thiophenecarboxamide), occurs via reduction of proinflammatory cytokines and antigen-induced T cell proliferation. *J Pharmacol Exp Ther*. 2005;312:373–381.
36. Mangelsdorf DJ, Thummel C, Beato M, et al. The nuclear receptor superfamily: the second decade. *Cell*. 1995;83:835–839.
37. Evans RM. The steroid and thyroid hormone receptor superfamily. *Science*. 1988;240:889–895.
38. Heyman RA, Mangelsdorf DJ, Dyck JA, et al. 9-cis retinoic acid is a high affinity ligand for the retinoid X receptor. *Cell*. 1992;68:397–406.
39. Tavera-Mendoza L, Wang TT, Lallemand B, et al. Convergence of vitamin D and retinoic acid signalling at a common hormone response element. *EMBO Rep*. 2006;7:180–185.
40. Jiménez-Lara AM, Aranda A. Vitamin D represses retinoic acid-dependent transactivation of the retinoic acid receptor-beta2 promoter: the AF-2 domain of the vitamin D receptor is required for transrepression. *Endocrinology*. 1999;140:2898–2907.
41. Ma F, Fuqua BK, Hasin Y, et al. A comparison between whole transcript and 3' RNA sequencing methods using Kapa and Lexogen library preparation methods. *BMC Genomics*. 2019;20:9.
42. Kim JA, Ahn D, Kim BY, Choi YJ, Shin HJ, Jan SY. Characterisation of human orbital fibroblasts cultivated from intracanal, nasal and central adipose tissues. *Br J Ophthalmol*. 2019. doi:10.1136/bjophthalmol-2018-313699
43. Fatourechi V, Pajouhi M, Fransway AF. Dermopathy of Graves disease (pretibial myxedema). Review of 150 cases. *Medicine (Baltimore)*. 1994;73:1–7.
44. Roos TC, Jugert FK, Merk HF, Bickers DR. Retinoid metabolism in the skin. *Pharmacol Rev*. 1998;50:315–333.